International Journal of Nanoelectronics and Materials
IJNeaM
ISSN 1985-5761 | E-ISSN 2232-1535

Analytical hierarchy process-based preliminary screening of rice husk-derived calcium silicate synthesis parameters using lauric acid adsorption

Zainor Syahira Zainal[a], Pengyong Hoo[a,b*], Siti Kartini Enche Ab Rahim[a,b], Abdul Latif Ahmad[c], Ahmad Zuhairi Abdullah[c], Qihwa Ng[a,b], Siewhoong Shuit[d], and Siti Zullaikah[e]

[a]*Faculty of Chemical Engineering & Technology, Universiti Malaysia Perlis, 02600 Arau, Perlis, Malaysia*
[b]*Centre of Excellence for Frontier Materials Research (CFMR), Universiti Malaysia Perlis, 02600 Arau, Perlis, Malaysia*
[c]*School of Chemical Engineering, Engineering Campus, Universiti Sains Malaysia, 14300 Nibong Tebal, Pulau Pinang, Malaysia*
[d]*Department of Chemical Engineering, Lee Kong Chian Faculty of Engineering & Science, Universiti Tunku Abdul Rahman, Sungai Long Campus, Jalan Sungai Long, Bandar Sungai Long, Cheras, 43000, Kajang, Selangor, Malaysia*
[e]*Department of Chemical Engineering, Faculty of Industrial Engineering, Institut Teknologi Sepuluh Nopember, Surabaya 60111, Indonesia*
** Corresponding author. Tel.: +60-12-916 0555; e-mail: pengyong@unimap.edu.my*

Received 10 May 2026, Revised 25 May 2026, Accepted 5 June 2026

ABSTRACT

With the increasing global demand for cleaner fuels, the use of biodiesel has grown steadily. As a potential feedstock, waste frying oil (WFO) is highlighted due to its availability and suitability for mild transesterification processing. As a low-cost and eco-friendly adsorbent, rice husk-derived silicates offer a promising strategy for waste frying oil polishing, specifically free fatty acid (FFA) content reduction. Upon this, lauric acid (LA) was used as a simplified model FFA to evaluate the calcium silicate performance under controlled conditions. Considering both production yield and adsorption capacity, the Analytical Hierarchy Process (AHP) was used as a decision-support tool to screen and prioritise all OFAT-based experimental data from four potential calcium silicate synthesis parameters, including sodium hydroxide concentration (0.5 – 2.5 M), calcium nitrate concentration (0.5 – 2.5 M), leaching temperature (60 – 100 °C), and leaching time (1 – 5 hours). The screening analysis revealed that sodium hydroxide concentration (1.5 – 2.5 M), calcium nitrate concentration (1.5 – 2.5 M), and leaching temperature (80 – 100 °C) strongly influenced both production yield and adsorption performance of calcium silicate. Under these highly prioritised ranks of synthesis conditions, the production yield of calcium silicates ranged from 58.77% to 83.48%, while the adsorption capacity ranged from 10.24 to 12.52 mmol/g. These results highlight the effectiveness of the OFAT analysis and AHP integration as a systematic preliminary screening-based method in prioritising the key parameters for subsequent synthesis condition optimisation. Indeed, it established a rational framework for the high-performance calcium silicate production for future WFO purification.

Keywords: *Waste frying oil; rice husk; calcium silicate; adsorption; Analytical Hierarchy Process*

1. INTRODUCTION

Biodiesel has emerged as a clean, renewable fuel in the current transportation sector due to its low carbon emissions and environmental sustainability [1]. Among the feedstock tested to improve the emission profile of biodiesel, WFO appeared to be one of the preferred choices due to its low economic value and often being discarded after repeated frying cycles [2]. However, its high FFA content led to soap formation that reduced biodiesel yield, requiring additional separation processes [3].

To overcome this issue, silica-rich rice husk ash (RHA) has shown potential to reduce FFA content from WFO through adsorption [4]. However, previous studies revealed that RHA achieved only 44% FFA removal due to its low specific surface area [5]. Beyond this limitation, the amorphous silica in RHA could be transformed into an advanced silicate-based adsorbent with improved characteristics, including an increased number of active adsorption sites, surface area, and pore structures [6]. Among these tested silicate-based adsorbents, alkaline earth metal silicates and plant-based calcium silicate were reported to be effective adsorbents for such purposes [7]. The superior performance was related to both production yield and adsorption performance, which were strongly influenced by the structural properties of the calcium silicate produced.

The synthesis process of calcium silicate could be divided into three main steps: i) RHA acid pretreatment; ii) Sodium hydroxide (NaOH) leaching to extract the pure silica from RHA into sodium silicate; iii) Calcium silicate precipitation using a calcium precursor such as calcium nitrate [8]. Among these three stages, sodium hydroxide leaching required critical control as it controlled the formation of sodium silicate, the main precursor of calcium silicate. Hence, its physicochemical properties significantly influenced its interaction with calcium ions during the subsequent precipitation stage, which in turn affected the structural properties and formation of calcium silicate.

On top of that, significant factors including the leaching agent concentration, temperature, and duration must be

controlled to ensure the high-quality sodium silicate formation [9, 10]. Furthermore, the precipitation stage also plays a significant role, as the concentration of calcium precursor dictates the interaction between silicates and calcium ions that would further drive the result of calcium silicate formation, structure and performance. Interestingly, the effect of NaOH concentration, typically studied within 0.5 – 2.5 M, showed that higher solution viscosity hinders the interaction of Na^+ ions with silica elements when extremely high concentrations are used [11]. When the same calcium precursor concentration range was applied, the cross-linking phenomena that limit the growth of the silicate chain were observed and attributed to the unbalanced ratio between the NaOH concentration and the calcium precursor [9].

On the other hand, improper leaching temperature control would result in the unwanted silica gel layer being formed and inhibit further silica dissolution [12]. It was reported that silica dissolution could occur effectively within 60 – 100 °C of leaching temperature, as the extremely high temperature caused a reduction in the rate of silica dissolution [13]. Furthermore, a prolonged leaching time influenced the extraction of crystalline silica, which limited the leaching agent's interaction with the available silica in RHA, hence slowing down the leaching process [14]. Previous studies reported that the amorphous silica extraction would occur within 1 – 5 hr [11, 15].

While the justification for these factors was well reported, their respective significance requires a systematic evaluation to ensure efficiency of further process optimisation that could control the resource utilisation of the adsorbent [8]. Without an effective preliminary screening, optimisation could require large experimental datasets and more computational effort for modelling accuracy [16, 17]. The current practice shows that the use of the one-factor-at-a-time (OFAT) preliminary screening method is commonly used due to its simplicity, but it cannot account for the interaction between variables [11]. For that reason, an intermediate strategy to enhance the robustness and consistency of the preliminary screening method needs to be focused on.

In this context, the AHP method was introduced as a systematic decision-support tool for preliminary screening that integrates both quantitative and qualitative judgment [12]. Such judgment systems facilitate the pairwise comparison with the use of a systematic hierarchy structure and a nine-point Saaty scale between selected factors [13]. The weight value of each criterion or response signals the logical coherence towards the final judgement of the factors (alternatives) involved [14]. Unlike the OFAT method, AHP provides a transparent and balanced screening framework that enhances the factor selection reliability and guides towards the subsequent conventional optimisation method. This approach could reduce the number of experiments by narrowing down the range of experimental conditions before detailed optimization conducted. Despite preliminary screening, the complexity of the WFO composition raised another concern for the adsorption studies. Other than complex FFA, the appearance of triglycerides, degradation products, and polymerised compounds might interfere with the adsorption system [18].

Among these aforementioned components, the reduction of FFA content from WFO remains a crucial step in enhancing the WFO quality, which could improve the efficiency of biodiesel conversion [19]. Hence, to assess the ability of rice-husk-derived calcium silicate, this study uses LA as the simplified FFA model representative of FFA content in WFO. The selection would represent a simplified system that enables control analysis of adsorbent performance with a simple FFA structure before extending the more complex system. Indeed, it could provide a reliable basis to determine the suitability of rice-husk-derived calcium silicate for real-world WFO application.

Nevertheless, this study uniquely integrates the AHP approach with the experimental data obtained from the OFAT method as a preliminary screening method that was not reported elsewhere. Such a method was employed to prioritise the significant synthesis factors and identify the influential operational ranges among NaOH concentration (0.5 – 2.5 M), calcium precursor (calcium nitrate) concentration (0.5 – 2.5 M), leaching temperature (60 – 100 °C) and leaching time (1 – 5 hr) to develop a high-performing calcium silicate, according to both production yield and adsorption performance criteria.

2. MATERIALS AND METHODS

2.1. Chemicals and materials

RH was obtained from Dibuk Sdn. Bhd., located in Kangar, Perlis. Calcium nitrate, $Ca(NO_3)_2$; sodium hydroxide, NaOH; hydrochloric acid, HCl; and isooctane, $(CH_3)_3CCH_2CH(CH_3)_2$, were all supplied in EMSURE® ACS grades and purchased from Biotek Abadi in Butterworth, Penang, Malaysia. The AR-grade potassium bromide (KBr) and lauric acid ($C_{12}H_{24}O_2$) were obtained from Kumpulan Saintifik F.E. Sdn. Bhd. (KSFE) in Petaling Jaya, Selangor, Malaysia. Unless explicitly stated, all chemicals and materials were used without further purification.

2.2. RH pretreatment

The raw RH was washed with distilled water to remove any attached dust and impurities before being dried in the oven at 100 °C for overnight. The washed RH was then subjected to the acid pretreatment using an HCl solution. In a typical pretreatment, 10 g of RH was refluxed at 60 °C in 100 mL of 3 M HCl for 3 hr, followed by a washing and filtering process using distilled water until the pH of the washed water became constant over three consecutive measurements. Once the washing process was done, the HCl-pretreated RH was dried in the oven at 100 °C for 12 hr before being combusted at 500 °C with a 5 °C/min rate for three hours in a Carbolite/CDF 15/1C furnace. The HCl-

pretreated RHA obtained after the calcination was ground and sieved using a mortar till the particle sizes were approximately 125 μm and kept in an airtight container until the next procedure.

2.3. OFAT experimental design

The experimental work started by investigating all synthesis parameters using the OFAT method, where each parameter was varied while other parameters remained constant. The factors investigated include NaOH and calcium precursor concentration, leaching temperature and time, as summarised in **Table 1.**

Table 1. List of synthesis parameters and their respective ranges

Synthesis parameters	Label	Unit	Value
NaOH concentration	A1	M	0.5
	A2		1.0
	A3		1.5
	A4		2.0
	A5		2.5
$Ca(NO_3)_2$ concentration	B1	M	0.5
	B2		1.0
	B3		1.5
	B4		2.0
	B5		2.5
Leaching temperature	C1	℃	60.0
	C2		70.0
	C3		80.0
	C4		90.0
	C5		100.0
Leaching time	D1	hr	1.0
	D2		2.0
	D3		3.0
	D4		4.0
	D5		5.0

Through this approach, both production yield and adsorption capacity were selected as key performance indicators of the screening.

2.4. Calcium silicate synthesis

For production yield, a typical calcium silicate synthesis was conducted, following a similar method to a previous study [20]. Specifically, 4.4 g of RHA was refluxed with 100 mL of 0.5 M NaOH solution at 100 ℃ with 200 rpm speed for 2 hr. The mixture was then filtered to separate silicate (SiO_3^{2-}) leachate from the RHA residual. The leachate obtained was then reacted with a calcium precursor, 70 mL of 1.0 M calcium nitrate, $Ca(NO_3)_2$ solution at 95 ℃ for 1 hr with continuous stirring under reflux. The precipitates formed were filtered and washed with distilled water before being dried at 100 ℃ overnight. The white precipitate obtained upon drying was the extracted calcium silicate. The steps were repeated for all synthesis parameters, following their defined operational ranges, using the OFAT principle and labelled as summarised in **Table 1**. The production yield of all calcium silicates obtained was then calculated using equation (1):

$$\text{Production yield} = \frac{m_{extraction}}{m_{initial}} \times 100\ \% \quad (1)$$

Where $m_{extraction}$ refers to the mass of calcium silicate obtained after drying, and $m_{initial}$ refers to the initial amount of RHA used in silicate extraction.

2.5. Batch adsorption setup

The adsorption capacity data were collected through LA batch adsorption. The 50 mmol/L of LA stock solution was first prepared by dissolving 10.02 g of LA in isooctane, and the solution was made up to 1 L using a volumetric flask. In a subsequent adsorption setup, 0.2 g of calcium silicate was added to 50 mL of 50 mmol/L LA solution that was filled in the conical flask. The flask of LA with the calcium silicate mixture was then placed on the orbital shaker at room temperature and allowed to shake for 10 min at 200 rpm. After the adsorption was ended, 1.5 mL of the sample mixture was taken out using a pipette and transferred into a 1.5 mL mini centrifuge tube for further separation using the microcentrifuge for 1 min at 10,000 rpm. After the mixture had successfully separated from the used adsorbent, 1000 μL of the solution was taken out using a micropipette and put into a 1.5 mL GC vial for gas chromatography-flame ionisation detector (GC-FID) analysis. These steps were repeated throughout all synthesised calcium silicates, and all experiments were run in triplicate.

2.4. Gas chromatography-flame ionisation detector (GC-FID) analysis setup

The GC-FID analysis was conducted using Agilent Technologies 7890B. The remaining LA separation from isooctane was attained using a non-polar column coated with 5 % phenyl-methyl polysiloxane, an Agilent HP-5 column (30 m × 0.25 μm × 0.25 μm). The initial oven temperature was set at 60 ℃ and increased to 325 ℃ with a 10 ℃ per min ramping rate and held for 5 min. The front detector and injector temperatures were fixed at 300 ℃ and 250 ℃, respectively. Meanwhile, for both sample injection and detection configuration, the LA sample was auto-injected via split-spitless (SSL) injector with a 20-split ratio and 80 mL per minute split flow. Helium (99.9995% purity) was used as the carrier gas in the system. Meanwhile, the FID was operated with synthetic air (99.999% purity) as an oxidiser to complete the combustion, hydrogen gas (99.9992% purity) as fuel and nitrogen gas (99.9995% purity) as the makeup gas to ensure a constant flow rate to the detector. The GC-FID results were then used to further observe and compare the adsorption capacities of LA achieved by all calcium silicates. The adsorption capacity was calculated using equation (2):

$$Q_t = \frac{(C_i - C_t)V}{W} \quad (2)$$

Where Q_t refers to the adsorption capacity (mmol/g), C_i refers to the LA acid initial concentration (mmol/L), C_t refers to the LA concentration in the solution at time t (mmol/L), V refers to the volume of LA sample used (L), and W refers to the adsorbent weight used (g/L).

2.7. Setup of AHP model for factor screening

All experimental data obtained from OFAT analysis were integrated into the AHP model. The AHP method was employed to prioritise and identify the key parameters for calcium silicate synthesis [21]. The method began with the hierarchical model structuring, which served as the core for evaluating the importance of various factors in achieving the main goal: prioritising synthesis conditions to synthesise calcium silicate. Subsequently, Saaty's 1 – 9 scale was used to determine the importance of selected criteria: adsorption capacity, Q_t, and production yield of calcium silicate. The relative importance scale decision was then used in establishing pairwise comparison matrices.

Following this, the consistency judgment of such an assessment was verified through the consistency ratio, CR. Once it was successfully verified, the overall priorities of potential alternatives that include sodium hydroxide and calcium nitrate concentrations, leaching temperature and time were calculated and analysed. Therefore, the failure of these assessments to meet the acceptable consistency would require the pairwise comparison matrices to be re-evaluated accordingly. The outcomes from AHP were then subsequently used as the guidance in further optimising the calcium silicate synthesis as an adsorbent. The flowchart of the overall steps involved is shown in **Figure 1**.

2.7.1. Problem identification and hierarchy structuring

The first step of the AHP method started with the main problem or goal of process determination, which involved a deep analysis towards potential key factors. Such a framework was connected through the tree-like structure of the hierarchy model development, as shown in **Figure 2**.

The hierarchy model structure was divided into three different levels that consist of the goal, criteria and alternatives. The first layer (yellow-highlighted) represented the goal, i.e., prioritising a range of synthesis conditions for calcium silicate, while the second layer (purple-highlighted) represented the criteria layer, which includes the indicators for synthesised calcium silicate, i.e., adsorption capacity, Q_t (mmol/g) and production yield (g/g RHA). The model is supported by the alternative layer (green-highlighted), in which all significant synthesis parameters, including NaOH concentration (0.5 – 2.5 M), precursor (calcium nitrate, $Ca(NO_3)_2$) concentration (0.5 – 2.5 M), leaching temperature (60 – 100 °C), and leaching time (1 – 5 hr).

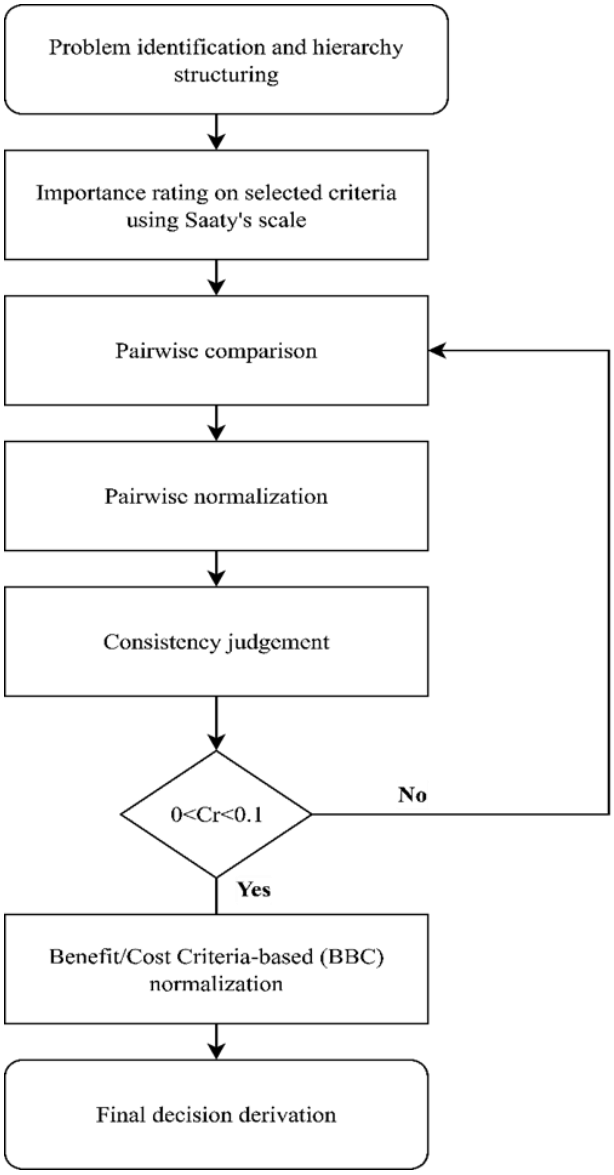

Figure 1. Flowchart of the overall steps involved in AHP

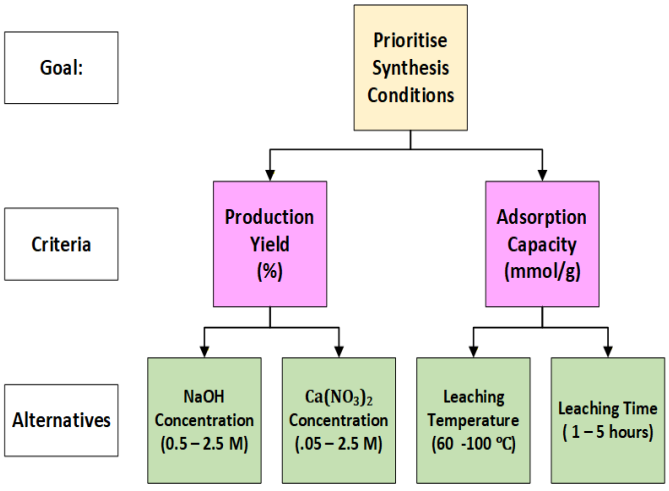

Figure 2. The hierarchical model developed in this study

2.7.3. Importance rating based on Saaty's scale

Saaty's 1–9 scales were applied in determining the importance level of adsorption capacity and production yield in achieving the primary goals of the process. The main values of the scale, which include 1 (equally important), 3 (moderately important), 5 (strongly important), 7 (moderately important), and 9 (extremely important), respectively, as each criterion is compared to the others [22]. Meanwhile, the intermediate values (2, 4, 6, 8) were used as the compromise judgment required between each criterion, and the reciprocal value (1/p) was used for the inverse comparison.

2.7.4. Pairwise comparison

The pairwise comparison was conducted after the importance level of each criterion had been identified. The comparison was done through the 2 × 2 matrices method, as tabulated in **Table 2,** with both selected criteria. Both the adsorption capacity and the production yield were compared with each row to the other column. In this study, the adsorption capacity, Q_t, was fixed to be three times more important than production yield, as this prioritisation highlighted the crucial role of higher adsorption capacity efficiency in LA removal. The weightage of the adsorption capacity, Q_t, and the production yield were calculated through the eigenvector approximation approach using equation (3):

$$W_j = \frac{1}{n}\sum_{j=1}^{n}\frac{a_{ij}}{\sum a_j} \quad (3)$$

Where w_j refers to the weightage of adsorption capacity and production yield, n refers to the number of criteria, a_{ij} refers to the element from the pairwise comparison matrices that compares the adsorption capacity and production yield/synthesis parameters row, i, to the adsorption capacity and production yield/synthesis parameters column.

Table 2. AHP pairwise comparison matrices table

Criteria	X1: Adsorption Capacity	X2: Production Yield
X1	1	3
X2	1/3	1

2.7.5. Pairwise normalisation

The consistency of scales used in previous pairwise comparisons of adsorption capacity and production yield was then validated through the pairwise normalisation method [13]. The pairwise normalisation was calculated using equation (4):

$$B_{ij} = \frac{a_{ij}}{\sum_{i=1}^{n} a_{ij}} \quad (4)$$

Where B_{ij} refers to the normalised value of that cell.

2.7.6. Consistency judgement

The consistency judgement was conducted to reveal the consistency and efficiency of the selected scale of both adsorption capacity and production yield after undergoing multiple pairwise comparisons. It was elucidated using the final value of consistency ratio, CR, in which a value below 10 % (CR < 0.1) indicated consistent comparisons and was acceptable for further processing [23]. Otherwise, the comparison was inconsistent, and the previous decision needed to be reviewed for the cause finding and corrective action [14]. CI and CR can be calculated using equations (5) and (6):

$$\text{Consistency index, CI} = \frac{\lambda_{max} - n}{n-1} \quad (5)$$

$$\text{Consistency ratio, CR} = \frac{CI}{RI} \quad (6)$$

Where λ_{max} represents the average values obtained by dividing the elements of all priorities matrix by the priorities vector, and RI refers to the random index that was determined according to the number of criteria.

2.7.7. Benefit/Cost Criteria-based normalisation

The benefit/cost criteria (BBC)-based normalisation was conducted as the final step in ensuring the adsorption capacity and production yield have correctly and fairly contributed to the final ranking of each synthesis parameter of calcium silicate [24]. For a BBC-based normalisation method, the higher values obtained for both adsorption capacity and production yield were crucial [25]. With the use of experimental data of both production yield and adsorption capacity, BCC-based normalisation can be calculated using equation (7):

$$r_{ij} = \frac{Max(x_{ij})}{\sum_{i=1}^{m}(x_{ij})} \quad (7)$$

Where r_{ij} refers to the rating value of normalised performance, $Max(x_{ij})$ refers to the maximum data value of synthesis parameters used, x_{ij} refers to the experimental data value of synthesis parameters used, i with respect to the production yield and adsorption capacity, j.

2.7.8. Final decision derivation

In the last step, the final ranking of each synthesis parameter with its respective operational range was determined using the preference weightage, wj, which served as the basis of the process, and the normalised performance rating, r_{ij}. The best synthesis parameter and its operational range were decided according to the high values obtained [12]. The calculation can be done using equation (8).

$$V_i = \sum_{j=1}^{n} w_j r_{ij} \quad (8)$$

Where V_i refers to the rank of each synthesis parameter of calcium silicate.

3. RESULTS AND DISCUSSION

3.1. Effect of leaching agent concentration

As different NaOH concentrations were used in the synthesis, two different trends were observed for the production yield and the adsorption capacity, as shown in **Figure 3**. According to **Figure 3**, the production yield of calcium silicates increased from 35.95 ± 0.05 % to 48.55 ± 0.03 %, then to 58.77 ± 0.10 %, 68.94 ± 0.43 % and 83.48 ± 2.05 %, when the NaOH concentration was increased from A1 (0.5 M) to A5 (2.5 M). Such an upward trend was attributed to the change in silica solubility at different concentrations. Higher NaOH concentration increased the solubility of the silica, allowing more sodium silicate leachate to be formed with a higher silicate anion ratio [26]. Consequently, improving the reactivity between the silicate and the calcium cations (Ca^{2+}) increased the precipitate yield at the end of the reaction [27].

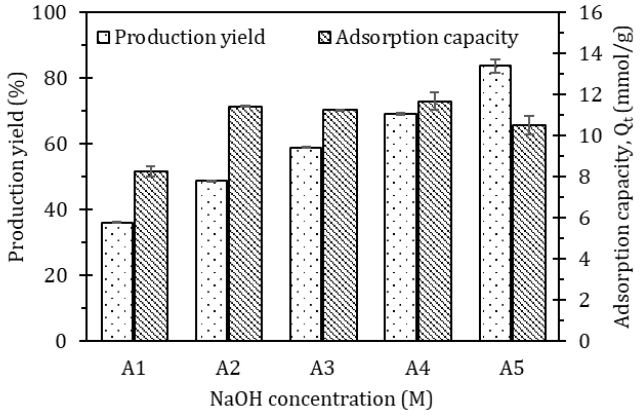

Figure 3. Production yield and LA adsorption capacity, Q_t, of calcium silicates using different NaOH concentrations at 100 °C for 3 hr, and 1.0 M $Ca(NO_3)_2$ at 95 °C for 1 hr.

Interestingly, the LA adsorption capacity revealed a different trend. The LA adsorption capacity increased from 8.2292 ± 0.25 mmol/g to 11.3927 ± 0.02 mmol/g when 1.0 M NaOH (A2) was used instead of 0.5 M (A1). At 1.5 M NaOH (A3), the LA adsorption capacity decreased slightly to 11.2126 ± 0.01 mmol/g before reaching the highest LA adsorption capacity of 11.6415 ± 0.43 mmol/g, revealed at 2.0 M NaOH (A4). The LA adsorption capacity drastically reduced to 10.4704 ± 0.45 mmol/g when the NaOH concentration was further increased to 2.5 M (A5). As previously described, higher NaOH concentrations could extract higher sodium silicate, allowing the enhancement of longer silicate chains that provided more binding sites for Ca^{2+} [15]. On the other hand, an aqueous environment would influence the deprotonation of LA molecules to form carboxylate ions, which then would exhibit their interaction with Ca^{2+} cations through electrostatic attraction [28].

Thus, it was understood that while a constant weight of the calcium silicates was used throughout the experiments, different NaOH concentrations would lead to structural differences. The higher NaOH concentration was expected to extend the silicate chain, providing more available sites for Ca^{2+} cation incorporation. Such conditions could enhance the attraction of carboxylate anions from LA molecules, increasing the adsorption capacity. However, the trend observed in **Figure 3** also hinted at a limitation at the highest NaOH concentration. The extremely high concentration potentially formed an excessive amount of sodium silicate, which then would act as a binding agent along the calcium silicate chain, disrupting the calcium silicate formation [29]. Thus, it potentially hindered the interaction between the Ca^{2+} cation and LA molecules, ultimately reducing the adsorption rate.

3.2. Effect of precursor concentration

As the second parameter, the precursor concentration used at the precipitation stage was hypothesised to significantly affect the production yield and adsorption performance of the calcium silicates. Such a hypothesis was tested with the trends illustrated in **Figure 4.**

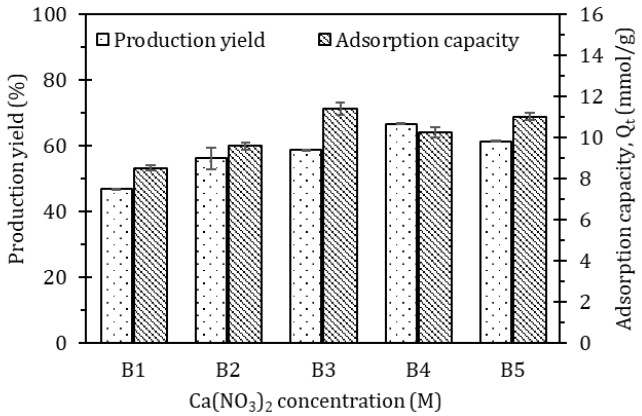

Figure 4. Production yield and LA adsorption capacity, Q_t, of calcium silicates using 0.5 M NaOH concentration at 100 °C for 3 hr, with different $Ca(NO_3)_2$ concentrations at 95 °C for 1 hr.

According to **Figure 4**, the production yield of calcium silicates increased from 46.77 ± 0.15 % to 56.13 ± 3.36 %, followed by 58.77 ± 0.01 % to 66.67 ± 0.24 %, as the $Ca(NO_3)_2$ was increased from B1 (0.5 M) to B4 (2.0 M), respectively. Interestingly, such an increment stopped at B4, as the production yield at B5 (2.5 M) reduced to only 61.30 ± 0.11 %. The observed trend could be attributed to the supersaturation phenomenon. The rate of particle nucleation and crystal formation enhancement within porous media was significantly influenced by a higher supersaturation of salt solution [30]. Therefore, at higher $Ca(NO_3)_2$ concentrations, higher Ca^{2+} cation concentrations were introduced to the sodium silicate solution, thus increasing the supersaturation level of calcium silicate. As the supersaturation level of the solution increased, the

nucleation rate of the solution increased, resulting in more calcium silicate precipitation.

Besides that, the cross-linking phenomenon could have occurred in this study, too. It was reported that the appearance of higher metal cation concentration within the silicate structure would encourage the cross-linking between the silicate chains, thus hindering the growth of silicate chains [29]. In fact, this study showed that a higher Ca^{2+} cation concentration would allow a more branched and interconnected silicate network, resulting in lower precipitate formation with a densely packed structure and limited pore size [31]. Such an elucidation justified the observed trend as the concentrations were increased from B1 to B5.

A fluctuating trend for the LA adsorption capacity was reported when different precursor concentrations were used. Initially, the LA adsorption capacities increased as the concentration of $Ca(NO_3)_2$ was increased from B1 (8.5164 ± 0.13 mmol/g) to B2 (9.5689 ± 0.19 mmol/g) and B3 (11.3809 ± 0.30 mmol/g). The adsorption capacity then declined to 10.2429 ± 0.25 mmol/g at B4 before bouncing back to 11.0114 ± 0.17 mmol/g at B5. Nevertheless, the final increment was lower than the adsorption capacity obtained at B3. As mentioned in Section 3.1, at lower precursor concentrations, sodium silicate would be a limiting factor, allowing most of the introduced Ca2+ to bind to silicate structures, thereby forming effective binding sites for the uptake of the LA molecule. Meanwhile, as the precursor increased, the grain formation and layering structure might potentially form, as it has been reported to reduce the overall surface area of the synthesised calcium silicates [32]. Hence, it would limit the LA molecules' diffusion onto the adsorbent.

3.3. Effects of leaching temperature

While the leaching agent concentrations reflected a dominant role, **Figure 5** reflects a fluctuating trend in calcium silicate extraction and performance across the leaching temperatures used.

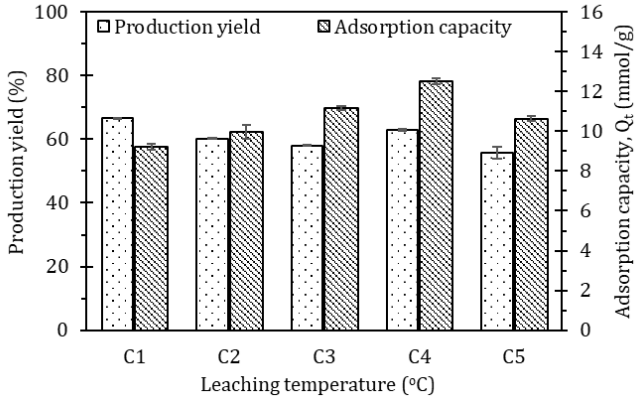

Figure 5. Production yield and LA adsorption capacity, Q_t, of calcium silicates using 0.5 M NaOH at 100 °C for 3 hrs, and 1.0 M $Ca(NO_3)_2$ with different leaching temperatures for 1 hr.

The highest production yield, 66.67 ± 0.15 %, was observed at the lowest leaching temperature, C1 (60 °C). As the leaching temperatures were increased to C2 (70 °C) and C3 (80 °C), the production yield decreased to 60.27 % ± 0.24 and 58.09 ± 0.10 %, respectively. The production yield then slightly increased to 62.93 ± 0.36 % at C4 (90 °C) before reducing to 55.73 ± 1.82 % at C5 (100 °C). In elucidating such behaviour, it was suggested that the higher production yield at C1 was due to rapid silica dissolution. The higher silica dissolution has been reported to allow more silica to interact with Na^+ cations from the NaOH solution, ultimately forming sodium silicate [33]. Consequently, higher sodium silicate concentration results in the formation of silicate monomers to a greater extent, favouring cross-linking between the silicate chains at the precipitation stage [15].

Meanwhile, the fluctuating trend of production yield could be related to the viscosity of the solution at higher temperatures. The higher leaching temperature would lower the mass transfer barrier between acid-pretreated RHA and the NaOH solution, which promotes the free movement of the silica and allows their effective interaction with the leaching agent [34]. Besides, higher leaching temperatures could also potentially influence the kinetic energy of the surrounding molecules, which have been reported to weaken the Si-O bond, thus disrupting the overall stability of the silicate structure [35]. However, the lowest production yield at C5 was attributed to the effective condition of silica degradation. At the highest leaching temperature, sufficient thermal energy to overcome the Si-O-Si bond dissociation energy could have been achieved, thereby promoting further silica degradation and inhibiting calcium silicate precipitation [36].

Moving to the LA adsorption capacity, the LA adsorption capacity was initially increased with the increased leaching temperature, from 9.2283 ± 0.13 mmol/g (C1) to 9.9636 ± 0.35 mmol/g (C2), 11.1610 ± 0.01 mmol/g (C3) and 12.5161 ± 0.15 mmol/g (C4), before being reduced to 10.6476 ± 0.12 mmol/g at C5. It was elucidated that more silicate monomers were formed at a lower leaching temperature. Thus, more Ca^{2+} cations would have been bonded in calcium silicate structures, providing more binding sites for carboxylate ions of LA molecules [37]. However, due to limited silica dissolution at higher temperatures that would lead to structural disruption, a more rigid structure could be formed and reduce the open structure, which is crucial in supporting the LA molecules' diffusion [38].

3.4. Effect of leaching time

Besides the leaching temperature, **Figure 6** revealed that the leaching time exhibits a minimal impact on both production yield and adsorption capacity of calcium silicates. Based on **Figure 6**, the production yield increased from 62.27 ± 0.10 % to 64.48 ± 0.53 %, as the leaching time increased from D1 (1 hr) to D2 (2 hr) but decreased to

61.19± 0.23 % when the leaching time was prolonged to D3 (3 hr). The production yield has moderately increased to 65.29 ± 1.40 % at D4 (4 hr) leaching time before reducing to 63.74 ± 0.69 at D5 (5 hr). Theoretically, a longer leaching time was required for deeper penetration of NaOH solution to allow more silica dissolution and increase sodium silicate concentration [26].

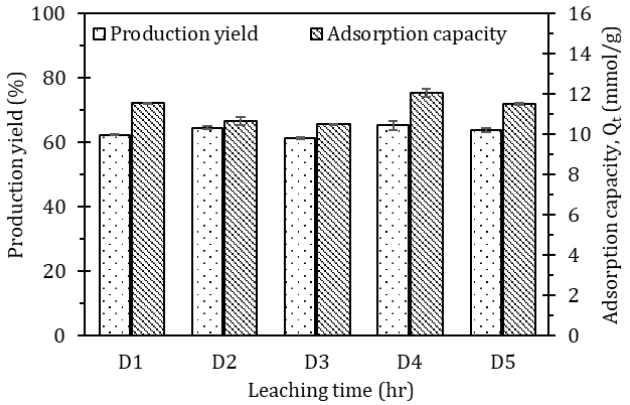

Figure 6. Production yield and LA adsorption capacity, Q_t, of calcium silicates using 0.5 M NaOH at 100 °C for 3 hrs, and 1.0 M $Ca(NO_3)_2$ at 95 °C using different leaching times.

Nevertheless, an interesting result was found in this study, which might involve two phases of silica extraction throughout the leaching times. At the initial leaching phase from D1 (1 hr) to D2 (2 hr), most of the amorphous silica from HCl-pretreated RHA could have been dissolved into sodium silicate [63]. As the leaching time prolonged, the dissolution of amorphous silica might approach the saturation state and start to involve crystalline silica, as a longer time was required to dissolve its ordered atom arrangement [39]. Therefore, the saturation phase could be approached with a longer leaching time as the concentration gradient of silica between the medium and its source had reduced, ultimately limiting the NaOH solution's penetration into HCl-pretreated RHA [40].

Similarly, LA adsorption exhibited a similar trend to the production yield. The LA adsorption capacity reduced from 1 hr (11.5374 ± 0.01 mmol/g) to 2 hr (10.6480 ± 0.18 mmol/g) and 3 hr (10.4862 ± 0.02 mmol/g). The adsorption capacity then increased when the leaching time was increased to 4 hr (12.0534 ± 0.19 mmol/g) before it declined to 11.5115 ± 0.04 mmol/g at a 5 hr leaching time. As previously discussed, prolonged leaching time could enhance silica dissolution, which allowed a more open structure in calcium silicates until saturation limits were approached while achieving higher uptake of LA molecules.

3.5. Priority screening using the AHP method

Table 3 shows the priority ranks of synthesis parameters determined using the OFAT experimental data that integrated with AHP-weighted production yield (0.25) and adsorption capacity (0.75). According to Table 3, the priority ranking was heavily influenced by the adsorption capacity due to its higher weightage (0.75) compared to the production yield weightage (0.25). Such a difference reflected the selection of adsorption capacity to be three times more important than production yield, which is consistent with the previous AHP studies, where adsorption performance appeared as the main functional adsorbent criterion [12]. Throughout this adsorption capacity domination, the calcium silicate synthesis conditions with higher adsorption capacity could achieve higher priority ranks, even with their comparatively moderate production yield. Moreover, the AHP rank reliability was validated through the CR value (0.001), in which a value below 0.1 indicates that the pairwise comparison matrix was consistent and the analysis was reliable [21]. Throughout these trends, it could be seen that calcium silicate produced using the higher NaOH and $Ca(NO_3)_2$ concentrations and leaching temperatures were ranked with the highest priority. Meanwhile, the priority rank of the leaching time factor shows a fluctuating trend.

Table 3. Summary of priorities in selecting the most influential range of synthesis conditions of calcium silicate

Synthesis parameter	Weightage		Priority
	0.2500	0.7500	
	Production yield (%)	Adsorption capacity (mmol/g)	
A1	35.9520	8.2292	0.6378
A2	48.5500	11.3927	0.8794
A3	58.7740	11.2126	0.8984
A4	68.9350	11.6415	0.9564
A5	83.4800	10.4704	0.9246
B1	46.7740	8.5164	0.7366
B2	56.1330	9.5689	0.8411
B3	58.7740	11.3809	0.9704
B4	66.6670	10.2429	0.9250
B5	61.3020	11.0114	0.9555
C1	66.6670	9.2284	0.8030
C2	60.2660	9.9636	0.8230
C3	58.0880	11.1610	0.8866
C4	62.9320	12.5161	0.9860
C5	55.7300	10.6476	0.8470
D1	62.2670	11.5374	0.9563
D2	64.4830	10.6480	0.9094
D3	61.1900	10.4862	0.8868
D4	65.2920	12.0534	1.0000
D5	63.7420	11.5115	0.9603

Note: A: NaOH concentration (0.5 – 2.5 M); B: $Ca(NO_3)_2$ concentration (0.5 – 2.5 M); C: Leaching temperature (60 – 100 °C); D: Leaching time (1 – 5 hr).

Specifically, the priority rank of NaOH concentration factors shows 1.5 M (A3) to 2.5 M (A5) as the most influential range, with 58.77 to 83.48 % of production yield and 10.47 to 11.64 mmol/g of adsorption capacity. It suggests that the ideal NaOH concentration range to leach out the silica into soluble sodium silicate lies within 1.5 to 2.5 M. Similarly, $Ca(NO_3)_2$ concentration also reflects a

similar trend with 58.77 to 66.68 % of production yield and 10.24 to 11.38 mmol/g of adsorption capacity.

This suggests that the Ca^{2+} cations obtained within 1.5 M (B3) to 2.5 M (B5) of $Ca(NO_3)_2$ concentration would effectively interact with the silicate monomer of sodium silicate in producing calcium silicate with enhanced adsorptive capabilities. On the other hand, the priority rank revealed that the ideal leaching temperatures lie within 80 ℃ (C3) and 100 ℃ (C5) with 55.73 to 62.93 % production yield and 10.65 to 12.52 mmol/g adsorption capacity. Such a range could potentially influence the development of a longer silicate chain through the higher silica dissolution [33].

However, the leaching time factor reflects a different trend, as the higher priority rank was included at 1 hr (D1), 4 hr (D4) and 5 hr (D5), with 62.27– 65.29 % of production yield and 11.51 to 12.05 mmol/g adsorption capacity. Such a trend reflected an ideal time range for the dissolution of amorphous silica, which could be achieved in the first hour [40]. Once the saturation phase of amorphous silica dissolution was reached, the dissolution of available crystalline silica would take place over a prolonged time [32, 33]. Overall, Table 3 shows that a higher range of reagent concentration and temperature could bring major changes in both production yield and adsorption capacity.

4. CONCLUSION

This study has integrated OFAT with AHP as a preliminary screening method in prioritised synthesis parameters of calcium silicate. The results show NaOH concentration (1.5 – 2.5 M), $Ca(NO_3)_2$ concentration (1.5 – 2.5 M) and leaching temperature (80 – 100 ℃) as the most influential synthesis parameters, together with their respective operational ranges. Within these prioritised conditions, the calcium silicate production could achieve rates of 58.09 to 83.48%, with an adsorption capacity of 10.24 to 12.52 mmol/g. Therefore, these findings provide a useful basis towards further optimisation and support the production of high-performing calcium silicate for real waste frying oil utilisation as biodiesel feedstock.

ACKNOWLEDGMENTS

The authors would like to acknowledge the support from the Fundamental Research Grant Scheme (FRGS) under the grant number FRGS/1/2022/TK05/UNIMAP/02/11 from the Ministry of Higher Education Malaysia. Furthermore, sincere indebtedness and gratitude are addressed to the Universiti Malaysia Perlis (UniMAP).

REFERENCES

[1] A. Suhara *et al.*, "Biodiesel Sustainability: Review of Progress and Challenges of Biodiesel as Sustainable Biofuel," *Clean Technol.*, vol. 6, no. 3, pp. 886–906, Jul. 2024.

[2] Monika, S. Banga, and V. V. Pathak, "Biodiesel production from waste cooking oil: A comprehensive review on the application of heterogenous catalysts," *Energy Nexus*, vol. 10, p. 100209, Jun. 2023.

[3] G. P. Maniam, H. S. Lim, and N. Mat Hussin, "Effect of Free Fatty Acid on Transesterification of Waste Cooking Oil," *Curr. Sci. Technol.*, vol. 3, no. 1, pp. 57–63, May 2023.

[4] H. K. Okoro *et al.*, "Recent potential application of rice husk as an eco-friendly adsorbent for removal of heavy metals," *Appl. Water Sci.*, vol. 12, no. 12, p. 259, Dec. 2022.

[5] S. Nattaporn and T. Porjai, "Recovery of used frying palm oil by acidified ash from rice husk," 2015.

[6] P. U. Nzereogu, A. D. Omah, F. I. Ezema, E. I. Iwuoha, and A. C. Nwanya, "Silica extraction from rice husk: Comprehensive review and applications," *Hybrid Adv.*, vol. 4, p. 100111, Dec. 2023.

[7] Z. S. Zainal *et al.*, "Performance Assessment of Alkaline Earth Metal Silicates for Lauric Acid Removal: An Analytical Hierarchy Process (AHP) Approach," *Key Eng. Mater.*, vol. 1028, pp. 73–78, Oct. 2025.

[8] D. Danaci, P. A. Webley, and C. Petit, "Guidelines for Techno-Economic Analysis of Adsorption Processes," *Front. Chem. Eng.*, vol. 2, p. 602430, Jan. 2021.

[9] S. Kumar and R. Jambulingam, "Statistical optimization of biodiesel production from the non-edible seed of Mimusops Elengi using RSM and ANN Studies," *Glob. NEST J.*, vol. 27, Feb. 2025.

[10] C. P. Kpadé, L. D. Tamini, S. Pepin, D. P. Khasa, Y. Abbas, and M. S. Lamhamedi, "Evaluating Multi-Criteria Decision-Making Methods for Sustainable Management of Forest Ecosystems: A Systematic Review," *Forests*, vol. 15, no. 10, p. 1728, Sep. 2024.

[11] H. Jabraoui, T. Charpentier, S. Gin, J.-M. Delaye, and R. Pollet, "Behaviors of sodium and calcium ions at the borosilicate glass–water interface: Gaining new insights through an *ab initio* molecular dynamics study," *J. Chem. Phys.*, vol. 156, no. 13, p. 134501, Apr. 2022.

[12] F. Wang and S. P. Yeap, "Using magneto-adsorbent for methylene Blue removal: A decision-making via analytical hierarchy process (AHP)," *J. Water Process Eng.*, vol. 40, p. 101948, Apr. 2021.

[13] S. Asra, Juanda, and N. Arpi, "Alternative location determination of frozen tuna industry using analytical hierarchy process (AHP)," *IOP Conf. Ser. Earth Environ. Sci.*, vol. 951, no. 1, p. 012082, Jan. 2022.

[14] H. Esen, "Analytical Hierarchy Process Problem Solution," in *Analytic Hierarchy Process - Models, Methods, Concepts, and Applications [Working Title]*, IntechOpen, 2023.

[15] J. Liu, C. Xie, C. Fu, X. Wei, and D. Wu, "Hydrochloric Acid Pretreatment of Different Types of Rice Husk Ash Influence on the Properties of Cement Paste," *Materials*, vol. 13, no. 7, p. 1524, Mar. 2020.

[16] C. M. U-Dominic, J. C. Ujam, and N. Igbokwe, "Applications of Analytical Hierarchy Process (AHP)

and Knowledge Management (KM) Concepts in Defect Identification: A Case of Cable Manufacturing," *Asian J. Adv. Res. Rep.*, pp. 9–21, Aug. 2021.

[17] S. Frish, I. Talmor, O. Hadar, M. Shoshany, and A. Shapira, "Enhancing consistency of AHP-based expert judgements: A new approach and its implementation in an interactive tool," *MethodsX*, vol. 14, p. 103341, Jun. 2025.

[18] R. Singh, B. S. Dien, and V. Singh, "Response surface methodology guided adsorption and recovery of free fatty acids from oil using resin," *Biofuels Bioprod. Biorefining*, vol. 15, no. 5, pp. 1485–1495, Sep. 2021.

[19] I. B. Banković-Ilić, I. J. Stojković, O. S. Stamenković, V. B. Veljkovic, and Y.-T. Hung, "Waste animal fats as feedstocks for biodiesel production," *Renew. Sustain. Energy Rev.*, vol. 32, pp. 238–254, Apr. 2014.

[20] Z. S. Zainal *et al.*, "Plant-based calcium silicate from rice husk ash: A green adsorbent for free fatty acid recovery from waste frying oil," *Heliyon*, vol. 10, no. 4, p. e26591, Feb. 2024.

[21] A. Azari, R. Nabizadeh, A. H. Mahvi, and S. Nasseri, "Integrated Fuzzy AHP-TOPSIS for selecting the best color removal process using carbon-based adsorbent materials: multi-criteria decision making vs. systematic review approaches and modeling of textile wastewater treatment in real conditions," *Int. J. Environ. Anal. Chem.*, vol. 102, no. 18, pp. 7329–7344, Dec. 2022.

[22] Risfaheri *et al.*, "Sustainable production of high-purity amorphous silica from rice husk: A comparative study on the impact of fresh and reused hydrochloric acid leaching," *South Afr. J. Chem. Eng.*, vol. 56, p. 100848, Apr. 2026.

[23] W. Hu *et al.*, "A comprehensive evaluation of commercial activated carbon for key gasoline vapor removal based on the improved AHP method," *J. Environ. Chem. Eng.*, vol. 12, no. 1, p. 111829, Feb. 2024.

[24] A. R. Krishnan, M. R. Hamid, G. H. Tanakinjal, M. F. Asli, B. Boniface, and M. F. Ghazali, "An investigation to offer conclusive recommendations on suitable benefit/cost criteria-based normalization methods for TOPSIS," *MethodsX*, vol. 10, p. 102227, 2023.

[25] I. Z. Mukhametzyanov, "ReS-Algorithm for Converting Normalized Values of Cost Criteria Into Benefit Criteria in MCDM Tasks," *Int. J. Inf. Technol. Decis. Mak.*, vol. 19, no. 05, pp. 1389–1423, Aug. 2020.

[26] T. M. Setyoningrum, S. W. Murni, W. W. Nandari, and M. M. A. Nur, "Effect of sodium hydroxide concentrations and particle sizes on silica extraction from mineral rock obtained in Kalirejo village, Kokap, Kulonprogo, Yogyakarta," *Eksergi*, vol. 18, no. 1, 2021.

[27] Assawasaengrat, Pornrin Jintanavasan, and Prakob Kitchaiya, "Adsorption of ffa, soap and glycerin in biodiesel using magnesium silicate," *Chem. Eng. Trans.*, vol. 43, pp. 1135–1140, 2015.

[28] S. K. Shukla and A. Kumar, "Dissociation of Equimolar Mixtures of Aqueous Carboxylic Acids in Ionic Liquids: Role of Specific Interactions," *J. Phys. Chem. B*, vol. 119, no. 17, pp. 5537–5545, Apr. 2015.

[29] Y. Aysa-Martínez, S. Anoro-López, M. Cano, D. Julve, J. Pérez, and J. Coronas, "Synthesis of amorphous magnesium silicates with different SiO2:MgO molar ratios at laboratory and pilot plant scales," *Microporous Mesoporous Mater.*, vol. 317, p. 110946, Apr. 2021.

[30] E. D. Skouras, V. Sygouni, G. N. Constantinides, and C. A. Paraskeva, "Flow, Transport, and Controlled Sedimentation of Salt Solutions in Porous Formations with Enhanced Structural Properties," *Cryst. Growth Des.*, vol. 16, no. 11, pp. 6230–6238, Nov. 2016.

[31] D. Hou, H. Ma, and Z. Li, "Morphology of calcium silicate hydrate (C-S-H) gel: a molecular dynamic study," *Adv. Cem. Res.*, vol. 27, no. 3, pp. 135–146, Mar. 2015.

[32] M. H. Kaou, Z. E. Horváth, K. Balázsi, and C. Balázsi, "Eco-friendly preparation and structural characterization of calcium silicates derived from eggshell and silica gel," *Int. J. Appl. Ceram. Technol.*, vol. 20, no. 2, pp. 689–699, Mar. 2023.

[33] B. Rao *et al.*, "Surprisingly highly reactive silica that dissolves rapidly in dilute alkali (NaOH) solution even at ambient temperatures (25 °C)," *J. Clean. Prod.*, vol. 341, p. 130779, Mar. 2022.

[34] G. Chen, J. Wang, X. Wang, S.-L. Zheng, H. Du, and Y. Zhang, "An investigation on the kinetics of chromium dissolution from Philippine chromite ore at high oxygen pressure in KOH sub-molten salt solution," *Hydrometallurgy*, vol. 139, pp. 46–53, Jul. 2013.

[35] L. Lu, Y. Zhang, and B. Yin, "Structure evolution of the interface between graphene oxide-reinforced calcium silicate hydrate gel particles exposed to high temperature," *Comput. Mater. Sci.*, vol. 173, p. 109440, Feb. 2020.

[36] F. M. M. Neto *et al.*, "Considerations on the effect of temperature, cation type and molarity on silica degradation and implications to ASR assessment," *Constr. Build. Mater.*, vol. 299, p. 123848, Sep. 2021.

[37] X. Guo and J. Wang, "A general kinetic model for adsorption: Theoretical analysis and modeling," *J. Mol. Liq.*, vol. 288, p. 111100, Aug. 2019.

[38] N. Rameli, K. Jumbri, R. A. Wahab, A. Ramli, and F. Huyop, "Synthesis and characterization of mesoporous silica nanoparticles using ionic liquids as a template," *J. Phys. Conf. Ser.*, vol. 1123, p. 012068, Nov. 2018.

[39] K. Gong, T. Aytas, S. Y. Zhang, and E. A. Olivetti, "Data-Driven Prediction of Quartz Dissolution Rates at Near-Neutral and Alkaline Environments," *Front. Mater.*, vol. 9, p. 924834, Jul. 2022.

[40] Y. Lin, B. Yan, Y. Wen, Z. Liang, T. Fabritius, and Q. Shu, "Dissolution behavior of silica in molten CaO–SiO_2–Fe_2O_3–MgO–MnO slag," *J. Am. Ceram. Soc.*, vol. 105, no. 6, pp. 3774–3785, Jun. 2022.

[41] I. Nurhidayati, E. Tri Wahyuni, N. H. Aprilita, and S. R. Hermanto, "Effect of Stirring Time on Sodium Silicate Synthesis From Mount Kelud Volcanic Ash," *ALCHEMY*, vol. 9, no. 2, pp. 48–53, Oct. 2021.